

Mode behavior, waveguide losses, and gain of two-sectioned, coupled-cavity GaAs/(Al,Ga)As terahertz and mid-infrared quantum-cascade lasers

Manfred Giehler, Helmar Kostial, Rudolf Hey, and Holger T. Grahn

Paul Drude Institute for Solid State Electronics, Hausvogteiplatz 5–7, 10117 Berlin, Germany

Email: giehler@pdi-berlin.de

A two-sectioned, coupled-cavity (TSCC) laser consists of two subcavities (length L_1 and L_2), which are separated by a thin gap (width \ll wavelength of laser light). Therefore, the two subcavities are optically coupled. For interband TSCC lasers, effects of laser-mode monitoring, wavelength tuning, and self-pulsation of lasing have been studied. [1] Hvozda *et al.* [2] have observed single-mode operation for TSCC mid-infrared (MIR) quantum-cascade lasers (QCLs). We extend the investigation of the mode control, waveguide-losses, and gain measurements to terahertz (THz) TSCC QCLs, compare these results with those of MIR devices, and analyze the observed effects within a transfer matrix approach.

We investigate THz and MIR GaAs/(Al,Ga)As QCLs with designs according to the ones introduced by Barbieri *et al.* [3] and Page *et al.* [4], respectively. The gap with a width of (350 ± 50) nm is formed by cleaving the laser ridge and refilling it with photoresist. The QCLs operate in a pulsed mode (width 100 ns). Time-integrated laser spectra were recorded using Fourier spectroscopy (spectral resolution 0.12 cm^{-1}) at 8 K.

The solid lines in Fig. 1 show typical mode spectra of THz TSCC QCLs for the case where both subcavities lase simultaneously. For THz devices, we observe the following mode features: First, the spacing between all modes is determined by the total length of both subcavities $\Delta\nu_{\text{all}} = 1/[2n_{\text{eff}}(L_1 + L_2)]$, where $n_{\text{eff}} = 3.71$ denotes the effective refractive index of QCLs in the THz region. Second, the mode heights exhibit a periodic modulation, and the period depends on the ratio L_2/L_1 ($L_2 > L_1$). Between modes of high intensity (in the following called major modes) indicated by circles in Fig. 1(a) for sample A with $L_2/L_1 = 1.2$, a certain number of modes is suppressed, which is determined by L_2/L_1 . These suppressed modes are referred to in the following as minor modes. The mode spacing between the major modes is determined by $\Delta\nu_{\text{maj}} = \Delta\nu_{\text{all}}(1 + L_2/L_1)$. For sample A ($L_2/L_1 \approx 1$), we observe about one major mode followed by one minor mode [cf. Fig. 1(a)]. The determined mode spacing is $\Delta\nu_{\text{all}} = 0.0088 \text{ THz}$ and $\Delta\nu_{\text{maj}} = 0.020 \text{ THz}$. For sample B, where $L_2/L_1 = 3.7$, three to four modes are suppressed [cf. Fig. 1(b)], and we obtain $\Delta\nu_{\text{all}} = 0.0073 \text{ THz}$ and $\Delta\nu_{\text{maj}} = 0.033 \text{ THz}$.

The mode features of THz TSCC QCLs can be described by a transfer matrix approach. $T_{ij}(\nu)$ denotes a wavenumber-dependent element of the transfer matrix, which takes into account all reflected and propagating partial waves during their round trip within the optically coupled subcavity 1–gap–subcavity 2 resonator. Assuming furthermore that each photon emission due to an intersubband transition is not affected by all others photon emission processes, the modes of a TSCC resonator are described by:

$$P(\nu) = |T_{22} + r_1 T_{21} + r_2 T_{12} - r_1 r_2 T_{11}|^2, \quad (1)$$

where $r_i(\nu)$ denotes the reflection coefficient of the facet i . Mode spectra for samples A and B calculated using Eq. (1) and $n_{\text{gap}} = 1.5$ are plotted in Fig. 1 by dotted lines. These spectra describe the mode spacings of the measured spectra well. Therefore, the mode control by selecting L_1 and L_2 can be explained by the interference of the laser light during its round trip within the TSCC resonator. In particular, the mode spacings obtained from the calculated spectra (sample A: $\Delta\nu_{\text{all,calc}} = 0.0088 \text{ THz}$, $\Delta\nu_{\text{maj,calc}} = 0.019 \text{ THz}$; sample

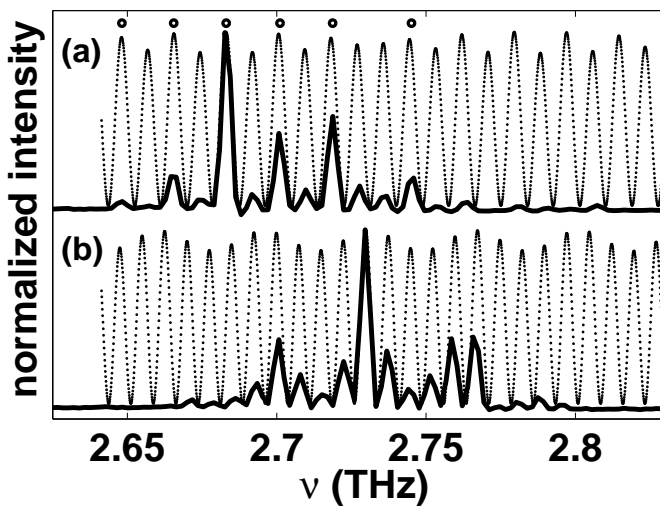


Fig. 1. Measured (solid lines) and calculated mode spectra [Eq. (1), dotted lines] of two THz TSCC QCLs. (a) sample A: $L_2/L_1 = 1.2$, $L_2 + L_1 = 4610 \mu\text{m}$, current $J_2 + J_1 = 1.24 \text{ A}$; (b) sample B: $L_2/L_1 = 3.7$, $L_2 + L_1 = 5400 \mu\text{m}$, $J_2 + J_1 = 2.2 \text{ A}$.

B: $\Delta\nu_{\text{all, calc}} = 0.0075$ THz, $\Delta\nu_{\text{maj, calc}} = 0.035$ THz) agree very well with the measured values given above. In contrast to the mode spacings, Eq. (1) does not describe the average value of the modulation degree $\eta = \langle (I_{\text{maj}} - I_{\text{min}}) / (I_{\text{maj}} + I_{\text{min}}) \rangle$ very well, where I denotes the mode height. Figure 1 shows that the calculated values are much lower than the measured ones. For sample A, we determine $\eta_{\text{calc}} = 0.023$ in contrast to $\eta_{\text{exper}} = 0.126$. Furthermore, η_{calc} does not strongly vary for different current values J_1 and J_2 , whereas η_{exper} clearly depends on J_1 and J_2 . We note that the irregularities in the modulation of the mode heights in the measured spectra are determined by the gain and loss spectra and are caused by random inhomogeneities within the laser ridge.

In contrast to THz TSCC QCLs, a larger manifold of mode features can be achieved for MIR devices by selecting appropriate values of J_1 and J_2 . As an example, Fig. 2 shows the spectra of a MIR TSCC QCL (sample C) for different delay times t between the current pulses through both subcavities. For subcavity 2, the current is somewhat below threshold, whereas for subcavity 1 the current is just above threshold. Therefore, for non-overlapping pulses ($t < -100$ ns and $t > +100$ ns), almost no lasing is observed. In Fig. 3, the laser intensity is plotted versus t . With slightly increasing overlap between both pulses (within $t \leq -90$ ns or $t \geq +30$ ns), the intensity increases (cf. Figs. 2 and 3) as expected. The maximum intensity is observed at -20 ns. For delay times of low and maximal laser intensity, the spectra are dominated by the major modes (cf. Fig. 2) with the spacing $\Delta\nu_{\text{maj}} = 1.125 \text{ cm}^{-1} \approx \Delta\nu_{\text{maj, calc}} = 1.165 \text{ cm}^{-1}$ using $n_{\text{eff}} = 3.34$. In contrast to the regions of low and maximum laser intensity, the laser intensity at $t = -70$ ns is remarkably decreased (cf. Fig. 3). At $t = -40$ and $+10$ ns (i.e., somewhat below and above the maximum intensity), the laser intensity is clearly reduced and exhibits a local minimum, respectively (cf. Fig. 3).

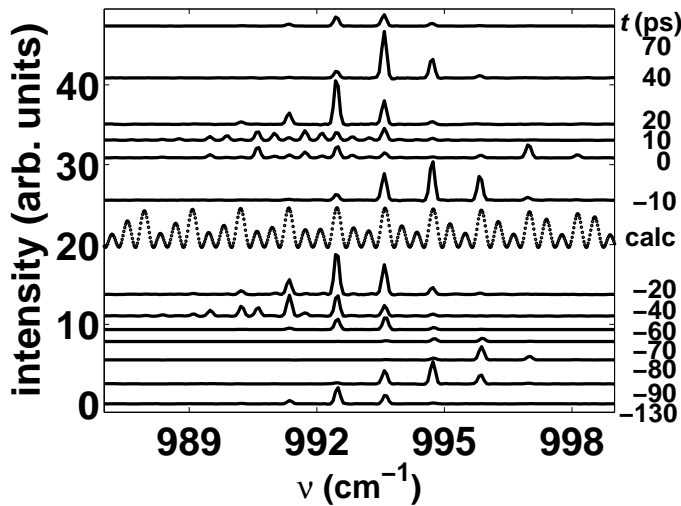


Fig. 2. Measured mode spectra (solid lines) of a MIR TSCC QCL (sample C: $L_2/L_1 = 2.1$, $L_2 + L_1 = 3960 \mu\text{m}$, $J_1(t) = J_2(0) = 0.9$ A, pulse width 100 ns) for different delay times. The dotted line shows a calculated spectrum as explained in the text.

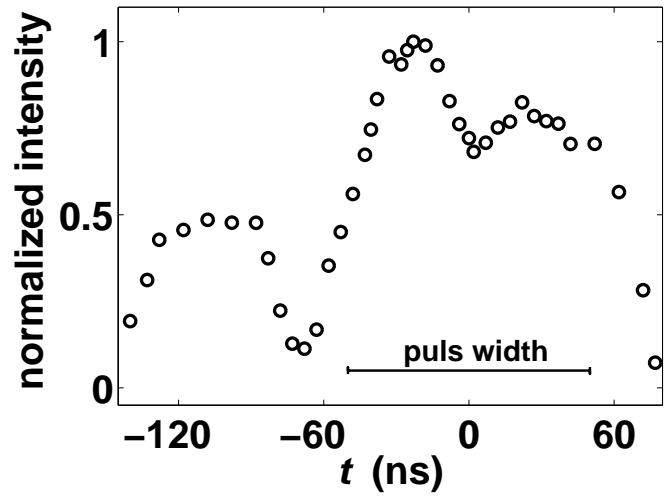


Fig. 3. Laser intensity of a MIR TSCC QCL (sample C) versus delay time between the current pulses through the two subcavities.

The peculiarities for -40 and $+10$ ns are reflected in the spectra by the appearance of all modes. The suppression is clearly removed (cf. Fig. 2). These spectra are similar to the ones of single-cavity lasers. We calculate $\Delta\nu_{\text{all, calc}} = 0.378 \text{ cm}^{-1}$, which agrees with the value of 0.371 cm^{-1} determined from the corresponding spectra. Figure 2 also shows a calculated mode spectrum for sample C assuming simultaneous lasing of both subcavities. Similar to the case of TSCC THz QCLs, the computed spectrum reproduces the spacing of the major modes, and the modulation of the mode heights is lower than observed. Finally, Fig. 2 shows that the frequencies of the modes do not shift with t , but different modes dominate the spectra for different delay times.

The main mode features of TSCC QCLs are the formation of major modes with the mode spacing $\Delta\nu_{\text{maj}} = \Delta\nu_{\text{all}}(1 + L_2/L_1)$ and the suppression of L_2/L_1 minor modes. These features are caused by interference effects within the TSCC resonator and can be well described by the transfer matrix approach in Eq. (1). The in part different mode behavior of THz and MIR devices might be caused by different wavelengths, waveguide losses, and gain of both types of QCLs. The observed modulation degree of the mode heights, its dependence on J_1 and J_2 , and the disappearance of the mode suppression (switching of the mode structure from that of a TSCC QCL to the one similar to a single-cavity laser) cannot be explained by Eq. (1) without taking into account the laser equations. Even for stimulated emission, the coupling between the photon densities and electron populations is not fully included in our model for a TSCC QCL.

REFERENCES

- [1] M. Radziunas, SPIE Proc. Series **4646**, 27 (2002).
- [2] L. Hvozdar *et al.*, Appl. Phys. Lett **77**, 1077 (2000).
- [3] S. Barbieri *et al.*, Appl. Phys. Lett. **85**, 1674 (2004).
- [4] H. Page *et al.*, Appl. Phys. Lett **78**, 3529 (2001).